ISSN: 2230-9926

Available online at http://www.journalijdr.com

IJDR

International Journal of Development Research
Vol. 12, Issue, 06, pp. 56685-56696, June, 2022

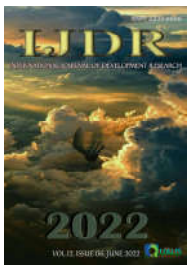

RESEARCH ARTICLE OPEN ACCESS

PERFORMANCE EVALUATION OF A PHOTOVOLTAIC SYSTEM WITH THE TWO-POSITION TRACKER IN THE CITY OF FORTALEZA, BRAZIL

***Felipe Teles, Francisco Samuel Portela Vidal, Elissandro Monteiro do Sacramento and Lutero Carmo de Lima**

Academic Master of Applied Physical Sciences, State University of Ceará, Fortaleza, CE 60740-000, Brazil

ARTICLE INFO

Article History:
Received 11th March, 2022
Received in revised form
21st April, 2022
Accepted 19th May, 2022
Published online 22nd June, 2022

Key Words:
Energy; Photovoltaic System,
Solar Tracking, Performance.

****Corresponding author:***
Felipe Teles

ABSTRACT

The present study evaluated a photovoltaic system with a tracker of two daily positions located at the State University of Ceará (UECE), Fortaleza, Ceará. A 50 W_p rated power system with a two-position manual tracker daily was compared with a fixed system at 0º in the horizontal plane. The results of the three stages of the experiment were collected in 16 days, in July/2021 and August/2021. Several data were collected, such as solar irradiation, electricity generated, and battery charge status. Other data were calculated from the data collected, such as reference productivity, the productivity of photovoltaic arrangement, the efficiency of photovoltaic arrangement, performance ratio (PR), and capacity factor (CF). The system with the two-position daily tracker generated 23.86% more electricity than the fixed system. In an additional comparison, a system with a manual tracker of 3 daily positions generated 29.89% more electrical energy than the fixed system. Finally, a simulation was performed in the Radiasol 2 program, seeking to perform a comparison similar to the practical experiment.

Citation: ***Felipe Teles, Francisco Samuel Portela Vidal, Elissandro Monteiro do Sacramento and Lutero Carmo de Lima.*** "Performance evaluation of a photovoltaic system with the two-position tracker in the city of fortaleza, Brazil*", International Journal of Development Research*, 12, (06), 56685-56696.

INTRODUCTION

The current climate crisis, pointed out by IPCC scientists, has led humanity to seek renewable sources of electricity, which are more environmentally sustainable, by emitting fewer greenhouse gases than fossil fuels. Electricity generation accounted for 36% of the world's energy sector's CO2 emissions in 2019 (IPCC, 2022, p. 9). The three primary renewable sources of electricity in the world are hydroelectric, wind, and solar, representing 16%, 5.5%, and 2.5% of the world's electricity matrix in 2019 (IPCC, 2022, p. 18). Photovoltaic solar energy has significant advantages over hydroelectric and wind sources. Hydroelectric power requires large floods of areas with vegetation, expensive and complex engineering projects, and the limitation of places with adequate relief for the construction of the plants. The environmental problem of flooding large areas with vegetation has been minimized by constructing Run-of-the-river (ROR) dams, which flood areas slightly more extensive than areas generally flooded in river flooding, and sought a better-installed power/flooded area ratio. However, the Run-of-the-river (ROR) dams are much more exposed to risks in the years that rain little in the hydraulic basins of the reservoirs, causing the generation of electricity to fall drastically.

In Brazil, the gradual inclusion of new ROR dams between 2010 and 2020 helped reduce the participation of hydroelectric plants in the country's electricity generation due to the low generation of water-wire plants in the drought years. The share of hydroelectric plants fell from 79.2% in 2010 (EPE, 2011, p. 45) to 63.8% in 2020 (EPE, 2021, p. 63). Wind power is only economically viable in areas with very high wind speed because electricity generation varies in the proportion of the wind speed hub. So if the wind speed drops by 10%, the electricity generation will fall by 27.1%. For this reason, the viable territorial area for wind power generation represents a small proportion of the total area of large countries such as Brazil. Moreover, because the generation varies to the cube of wind speed, the generation drops a lot in years of winds far below average. In Brazil, an exciting synergy happened between hydroelectric power and wind energy in the past decade. In the years of lower average rainfall in the country, there were above average winds, and in the years of weaker winds, the rains were heavier. Looking at the historical average, this synergy relationship is powerful. The big problem is if an isolated year happens with a "perfect storm," a year with weak winds and weak rains, which would be a disaster for a country so dependent on this synergy since hydroelectric generation accounted for 63.8% of wind generation and wind generation by 9.2% in 2020 (EPE, 2021, p. 63).

Photovoltaic solar generation depends on solar radiation and has significant advantages such as the abundance of availability and the slight variation of interannual generation. For comparison, Brazil has 8.51 million km² of area. At the same time, an area of only 2,500 km² covered with solar plants means 357,000 MW of installed power, considering a conservative ratio of 7 m² of an occupied area for each one kW_p of installed power (GREENVOLT, 2022). This power of 357,000 MW can generate 64,200 average MW of electricity if the average capacity factor is 18%, a value capable of being obtained in high-radiation areas of the country, even without solar tracking systems. The load of the National Interconnected System (SIN) of Brazil in 2020 was of the order of 66,700 average MW (EPE, 2021, p. 75), a value close to the above (64,200 average MW), that is, a small area of the national territory can supply almost all load of the SIN, provided that the problem of energy storage is solved. As for the annual variation, solar radiation has a more minor interannual variation than winds or rains, which is further reduced by the installation of power plants in different country regions.

The significant challenges of photovoltaic solar generation are the costs and its daily intermittence, and the generation is high in just 8 hours a day. Photovoltaics accounted for 99% of the world's installed solar power capacity in 2019, and the costs of generating electricity from the photovoltaic source fell by 56% between 2015 and 2020 (IPCC, 2022, p. 3). The daily intermittence can be compensated for by the synergy with hydroelectric and wind power plants, which operate at night, and by mature technologies such as pumped storage, which consume electricity at times of high solar generation and generate electricity at times of no solar generation. Reversible hydroelectric plants accounted for approximately 97% of the planet's installed capacity of electric energy storage systems (IRENA, 2017, p. 24). In the world, reversible hydroelectric plants reached 150 GW of installed and operational capacity at the end of 2016 (IRENA, 2017, p. 50). In the same year, the installed power of Brazil for all forms of electricity generation was 150.3GW (EPE, 2017, p. 33). A great way to increase photovoltaic electrical generation is by following the sun's direction during the day and the seasons. The more direct solar radiation is perpendicular to the plane of photovoltaic plates, the higher the incident radiation, positively impacting electrical generation. For analysis, in Brazil, 96% of the photovoltaic projects enabled in the A4 auction in 2018 were projects with solar followers (EPE, 2018, p. 26), a strong indicator of market confidence in solar followers technology its positive economic cost-benefit ratio. However, there are still doubts about the reliability of solar tracking technologies in the long term and the difficulty of inserting them in small and medium-sized projects. In large photovoltaic plants, the standard is using a single motor to rotate an axis with up to a hundred photovoltaic plates, which helps reduce the cost per module installed.

The main objective of this study is to evaluate the performance of a photovoltaic system with a two-position daily tracker with 45º East (azimuth angle of 90°, tiltangle of 45°) until the solar noon and 45º West (azimuth angle of -90°, tilt angle of 45°) from noon solar until the end of the day) in the city of Fortaleza, located in northeastern Brazil, focusing on constructive simplicity, and cost-benefit (even generating less energy than a system that follows the sun all day) so that it can be viable in small, medium and large photovoltaic systems. The system with tracker will be compared to a fixed system at 0° (azimuth angle of 0°, tiltangle of 0°) in the horizontal plane, in terms of electricity generation, and both systems will be constantly cleaned, because the system at 0° is not self-cleaningby the rain. An additional goal will be to compare the fixed system with a system of three daily positions in the exact location. In addition, other additional objectives are to evaluate four indicators of the fixed system at 0º in the horizontal plane (reference productivity, productivity of the photovoltaic arrangement, efficiency of the photovoltaic arrangement, and performance ratio) and an indicator in both systems (capacity factor). Finally, a simulation will be made in the Radiasol 2 software to evaluate the increase in radiation provided by the two-position system. The results will be used for future experiments in state of Ceará, Brazil.

Literature review: The Sun is located at the center of our solar system, and it is estimated that it will survive in the next 5 billion years (QUASCHNING, 2005, p. 44). This guarantees an inexhaustible energy source in the time scale of life on Earth (PEREIRA *et al*., 2017, p. 15),and considering the scale of humanity's energy consumption. The sun's radiation is generated by the process of nuclear fusion, where four hydrogen protons fuse to form a helium nucleus, two positrons and two neutrinos. The final mass of all particles is smaller than the mass before the reaction, and the mass difference is converted into energy (QUASCHNING, 2005, p. 45). Solar radiation enables indirect energy flows that sustain life on earth, and photovoltaic solar energy represents the flow of energy emitted by the Sun and transmitted in electromagnetic radiation (VIDAL, 2019, p. 22).

The Sun emits on each square meter of its surface a radiant power of 63.11 MW, and only 200,000 square meters of the Sun's surface emit in 1-year radiant energy equivalent to the total primary energy currently demanded on Earth in the same time interval (QUASCHNING, 2005, p. 47). However, the solar radiation that reaches each square meter from the top of the Earth's atmosphere is much smaller because of the distance between the Sun and the Earth. As this distance fluctuates during the year, the value of solar radiation varies by almost 7% in that time interval. The average value of solar radiation during the year at the top of the Earth's atmosphere is known as a solar constant and is equal to 1366 W/m² (PEREIRA *et al.*, 2017, p. 15). The power flow per area is specifically called solar irradiance. In contrast, the integral of irradiance in a time interval is explicitly known as solar irradiation, which is equivalent to the division of energy by the area. Solar radiation is converted into electrical energy through the photovoltaic cell, which constitutes the basic photovoltaic apparatus. The photovoltaic cell is composed of a PN junction, formed basically by silicon with the inclusion of some impurities in small amounts for electronic doping. A layer with boron or other trivalent impurity represents the type p semiconductor to facilitate a positive charge. In contrast, another layer is doped with phosphorus or another pentavalent impurity, representing the semiconductor type n, facilitating a negative charge (AWASTHI *et al*., 2020, p. 393). The electric field attracts excess electrons to the N region when the photovoltaic cell is illuminated by solar irradiance. In contrast, the gaps attract the P region, generating a potential difference. If each side of the joint is connected externally by metal terminals, an electric current is formed (ZILLES *et al*., 2012, p. 17).

To achieve commercially used voltage and current levels, a set of photovoltaic cells is connected to form a photovoltaic module with a rigid protective structure and a transparent top layer with anti-reflective glass (VIDAL, 2019, p. 34). The voltage and current values of photovoltaic modules depend on conditions such as the value of solar irradiance and the temperature of the modules. The nominal power of the photovoltaic module is obtained under standard test conditions (STC), 1000 W/m² of solar irradiance, photovoltaic cell temperature of 25 °C, and 1.5 air mass (AM). The rated power in watt-peak (W_p) has a maximum power current (IMP) and a maximum power voltage (VMP) (ZILLES *et al*., 2012, p. 20). Part of the Sun's rays that reach the Earth's atmosphere reach the Earth's surface in the same direction as the Sun, known as direct irradiance. In contrast, the atmosphere reflects another part and has no defined direction, known as diffuse irradiance.

The sum of the two irradiances represents global irradiance. From an observation point of the Earth's surface, which can be the plane itself where the photovoltaic solar system will be installed, the position of the Sun in the sky varies during the day and during the four seasons, which impacts the significant variation of the value of the angle formed between the plane of the photovoltaic system and the direct irradiance of the Sun. Solar followers seek to make the photovoltaic system plane as perpendicular as possible to the direct rays of the Sun to increase the incident irradiance. Direct irradiance represents most global irradiance, especially in regions of clean skies and high global irradiance. From the point of the observer on Earth, it is possible to see the projected motion of the Sun in a sphere with an arbitrary and

concentric radius to the Earth, called the celestial sphere (MORAIS, 2017, p. 25). The position of the Sun in the sphere is obtained from a two-angle coordinate system. The height or elevation of the Sun (alpha) is the angle formed between the Sun's radius and the sunbeam's projection over the observer's horizontal plane. The maximum solar elevation forms an angle of 90º. The azimuthal angle is the angle between the projection of the Sun's rays in the horizontal plane and the North-South direction from the observer's horizon (PINHO; GALDINO, 2014, p. 72). Point 0º is located in the geographic North.

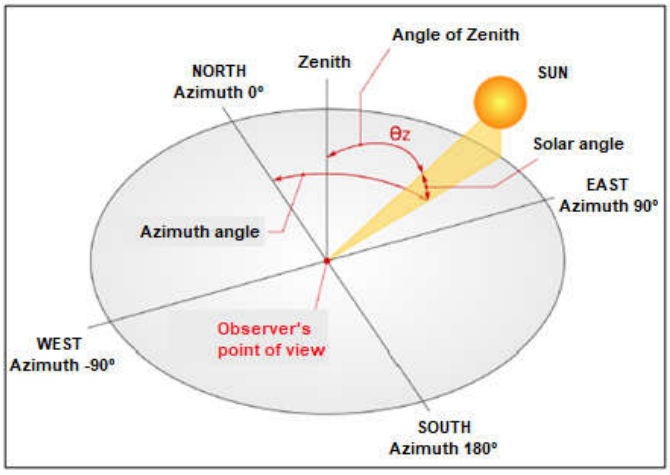

Fig. 1. Notable solar angles

The azimuthal angle varies between -180º and +180º, with the positive numbers being to the right of the geographic North. Finally, the zenith angle (Z) is formed between the Sun's radius and the Sun's projection over the observer's plane. Figure 1 shows the solar angles quoted from an observer's point of view on the ground. The higher the zenithal angle, the lower the level of solar irradiance that focuses on a surface of a photovoltaic module (CASTANEDA, 2011, p. 47), considering that the surface is perpendicular to the zenith (figure 1). When the direction of the Sun is not the normal line in relation to the surface of the photovoltaic module, the incident radiation per unit of area Gi will be reduced by the value of the cosine of angle i (CASTANEDA, 2011, p. 32), which is the angle formed between the surface normal and the direction of the Sun. When the module is installed at 0º horizontally, the zenith angle has the same value as the angle i. The Gn value represents the incident radiation on the surface of the Earth, perpendicular to the Earth's Sun's rays. The effective radiation incident in the photovoltaic module (Gi) is given by equation 1 (CASTANEDA, 2011, p. 32):

$$Gi = Gn \times \cos i \quad (1)$$

Thus, if angle i is 0º (half day, equinox day on the equator), the cosine of 0º is 1. When the solar ray is perpendicular to the normal of the photovoltaic module, the loss of direct radiation will be zero, so the incident radiation will be maximum. On the other hand, if angle i is 90º (end of the day), the direct radiation loss will be total, and the incident radiation will be equal to zero. Equation 1 has significant consequences, such as the fact that the losses are not proportional to the value of angle I, angle 15º has a cosine value of 0.966 (UFRGS, 2022), so the loss of radiation incident on a surface by misalignment of 15º about the direction of direct radiation of the Sun will be only 3.4%. On the other hand, a misalignment of 30º will represent a loss of 13.4% (cosine value equal to 0.864), and misalignment of 45º will mean a loss of 29.3% (cosine value equal to 0.707). What this shows is that solar trackers that minimize the misalignment of the average surface of the photovoltaic module about direct radiation from the Sun, with misalignment values less than 15º, will have a result very similar to almost perfect trackers that follow the direction of the Sun with misalignment less than 1º. Photovoltaic solar tracking systems seek to increase the generation of electrical energy by moving photovoltaic modules to make them perpendicular to the solar rays (DE SÁ CAMPOS; TIBA, 2021, p. 1). They are classified into five types based on their technologies: active, passive, semi-passive, manual, and chronological tracking (HAFEZ; YOUSEF; HARAG, 2018, p. 754).

The active system determines the sun's position from sensors, actuating motors, and gear mechanisms. Active trackers consume electricity but are more accurate and lead to a more significant increase in efficiency compared to passive systems. Active tracking systems can be based on microprocessors, auxiliary photovoltaic cells, and the date and time methods. Passive solar trackers use the sun's heat to generate an imbalance, generating tracker movement (SUMATHI *et al*., 2017, p. 130). They use a low boiling compressed gas fluid, packaged in 2 separate cylinders and interconnected by a tube. One cylinder is exposed to sunlight, and another is not exposed. The exposed cylinder generates fluid heating and increased pressure, causing the heated fluid to move to the other cylinder colder. This mass displacement creates an imbalance that causes the displacement of the structure. Passive trackers can stop working at low temperatures. Semi-passive solar trackers use a solar concentrator system formed by a Fresnel lens, a micro heliostat, and a receiver, which keeps the sun's rays perpendicular to the absorbing area with low mechanical effort (HAFEZ; YOUSEF; HARAG, 2018, p. 755).
The manual solar tracker changes the tilt angle by moving manual gears operated by a human. The factors that will strongly impact the viability of the manual system are the cost of labor and the number of angle changes per day. The chronological solar tracking system moves at a fixed rate, usually 15 degrees per hour, regardless of the day and month of the year. The chronological system achieves a good cost-benefit because it is more energy efficient than active systems, and the losses are only slightly higher than in active sensor-controlled systems.

As for the number of rotating shafts, solar trackers are classified into one-axis trackers and two-axis trackers. Single-axis trackers can be positioned horizontally, vertically, or inclined, with a north-south or east-west orientation (LIRA, 2014, p. 15). The 2-axis tracker has an axis that tracks the daily movement of the Sun and another that adjusts its inclination according to the seasons. The two-axis system achieves more significant power generation but has greater complexity and costs. The two-axis system is more suitable in systems that require high solar tracking accuracy, such as concentrated solar systems. As for the tracking strategy, the trackers are classified into polar, azimuth, and horizontal axis. The horizontal axis trackers perform well in regions close to the Equator (LIRA, 2014, p. 21) and are installed with a 0º inclination angle concerning the ground. The structure moves in the east-west direction, following the daily movement of the Sun, and often a single engine rotates a large number of photovoltaic modules. Horizontal axis trackers can also adopt the north-south direction to follow the seasons, but in this case, the gains are much smaller and are more viable in manual systems because they require few annual changes. The azimuthal tracker uses an impeller motor on the vertical axis, which causes the module to move east-west through rotation relative to the vertical axis. According to site latitude and season, the azimuthal system has a north-south orientation for manual tilt adjustment. They have good results in high latitudes, long days in summer, and the low cost of assembly and maintenance (OLIVEIRA, 2008, p. 10).

However, the azimuthal tracker has difficulty having the scalability of the horizontal axis tracker in large systems. The number of modules moved per engine is more diminutive. The polar tracker has a north-south fixation structure on an inclined axis. This axis tilt typically has the same value as the latitude of the installation location. The inclined axis follows the daily trajectory of the Sun in the east-west direction. In the polar tracker, the sun rays remain perpendicular to the photovoltaic module throughout the entire day of the spring and autumn equinoxes. For two days of the year, the losses due to misalignment are virtually negligible nil. On other days of the year, there is some loss of electricity generation, due to the error of the angle of incidence, with peak loss in winter and summer equinoxes.

Several studies focused on the construction of solar tracking systems of few positions a day, focusing on the cost-benefit of having results very close to those of very accurate algorithm systems, in terms of incident radiation, while having greater constructive simplicity. Huang and Sun (2007) developed a solar tracking system with 3 positions a day, 1 axis without concentration, and an additional system with a low concentration reflector. The analysis showed that the optimal angle in the morning and afternoon was 50º, facing east in the morning and west in the afternoon. The 3-position system generated an output increase of 24.5% compared to a fixed module at latitudes below 50º. In addition, a system of low concentration reflectors (2x) increased generation by 23% compared to a system without concentration. Combining the 3-position per day tracker with the low concentration reflector system, the power generation increase was 56%. Huang and Sun's 3-position solar tracker (2007) is in Figure 2 and uses an engine and a solar position sensor. The sensor consists of two photosensitive sensors, and the Sun's motion induces a shadow on one of the photosensitive elements. This shadow induces a signal that drives an engine to move to the next position. The experiment used an 85 W_p flat plate photovoltaic module [FMSN- 85W-R02] with 36 solar cells arranged in six arrangements.

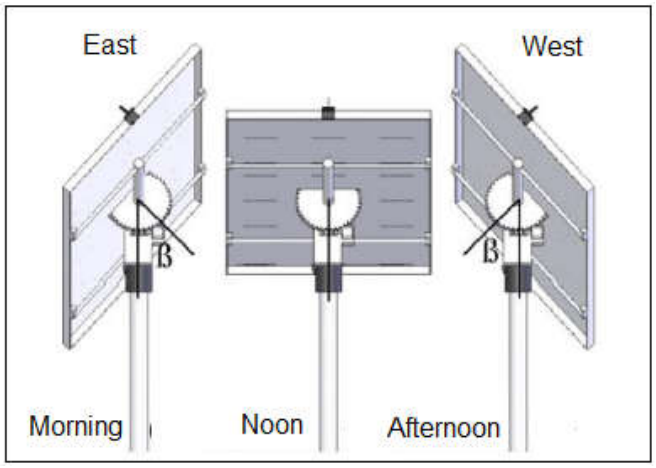

Fig. 2. Three-position Solar Tracker

Zhong *et al.* (2011) analyzed the optical performance of solar panels with a new solar tracking technique based on a proposed mathematical method and monthly horizontal radiation. The study showed that with the height angle of the solar panels adjusted daily three times in three fixed positions, east, south and west, morning, noon and afternoon, respectively, rotating the solar panels around the tilt angle. The calculation results showed that solar panels tracked 3 positions with a fixed annual tilt angle obtained a maximum annual harvestable radiation equivalent to 93% of the harvestable radiation in a 2-axis solar panel with accurate monitoring. The system with three angles per day in the east-west direction, and with 4 annual adjustments in the north-south direction (seasonal), the harvestable radiation was equivalent to 96% of the harvestable radiation of a 2-axis solar panel with precise monitoring. In the study, the soil albedo was considered to be 0.22, and the monthly horizontal radiation data used for calculations were taken from the average of monthly measurements from 1971 to 1999 at 32 locations in China, in locations with the most varied climatic conditions and a wide latitude range of the site.

Da Silva (2017) built a prototype with 2 movement axes (north-south and east-west), compared it with a fixed system, in order to obtain the percentage gain. The experiment was carried out in São Mateus, Espírito Santo, on the campus of the Federal University of Espírito Santo (UFES). The movement of the solar tracker was carried out with the aid of 2 DC 12 V motors with reduction box controlled by an Arduino Mega 2560 according to the light intensity that fell on the LDRs sensors. The system's automatic movements made it possible to adjust the position in relation to the sun throughout the day, in addition to placing the 55 W_p photovoltaic module horizontally for safety reasons at the beginning of each night. The prototype built with the solar tracker obtained an increase in energy generation of around 31.45% compared to the fixed system.

MATERIALS AND METHODS

The experiment was carried out at the State University of Ceará (UECE) - Brazil, located in the geographical coordinates 3º 79' of Latitude South (S) and 38º 55' West Longitude (W). The experiment made a comparison between two photovoltaic systems, one fixed and the other with a manual solar tracker. The two photovoltaic modules used in the experiment (figure 3) are from the Komaes brand, model KM50, with a nominal power of 50 W_p. The base system consists of a fixed photovoltaic module positioned at 0°. The second system was built with a module that is freely moved by a manual solar tracker, in the east-west direction, between 45º East and 45º West.

Fig. 3. Two photovoltaic modules installed

The fixation of the two solar modules took place in an iron structure, which was fixed to the ground. The Komaes KM50 module features under standard test conditions (STD) a maximum power voltage of 17.74 V, a maximum power current of 2.84 A, and a short circuit current of 3.04 A. It has 36 crystal cells, and the dimensions of each module are 750 mm x 510 mm x 35 mm, the mass is equal to 4.9 kg (SOLAR BRASIL, 2022). The incident solar radiation was obtained through a pyrometer located at PCD/FUNCEME station, close to where the modules were installed, just 85 meters away. The electrical part of the system was mounted in a small masonry room (figure 4) located 5 meters from the fixed system and 8 meters from the system with the manual solar tracker. Each system was connected to the structure mounted in the masonry room through 4mm² copper section wires. Inside the masonry room there is an independent electrical structure for each system: a wattmeter, a charge controller, a battery, a datalloger, and a set of LED lamps. The two batteries used were Heliar Freedom stationary batteries, one of which ismodel DF300 – 30Ah/26Ah (figure 5), used in Off Grid photovoltaic solar energy systems. Battery dimensions are 175mm long, 175mm wide and 175mm high, the mass is equal to 8.8 kg. The estimated useful life is more than 4 years, with a discharge depth of 20%.

Fig. 4. Masonry room where the electrical structure was built

The battery capacity is 30Ah in the discharge of 100 hours and 26 Ah in 20h discharge (NEOSOLAR, 2022). The voltage is 12V. The other battery is model DF500 – 40Ah/36Ah, with a mass of 9.7 kg, a discharge capacity of 40Ah in a 100-hour regime, and a discharge capacity of 36Ah in a 20-hour regime (NEOSOLAR, 2022). The larger battery has the same technology and the purpose of using the smaller battery and was used in the system of higher power generation, the system with the manual solar tracker of two positions and three daily positions, to prevent the battery from getting close to the maximum charge, and the system from running outside the Maximum Power Point Tracking (MPPT). The two charge controllers are EPEVER brand, and both have a rated load current of 10A and work with both 12V and 24V voltage. A controller is model TRIRON 1206N, with advanced MPPT algorithm control, with MPPT technology efficiency of not less than 99.5%, maximum DC/DC conversion of 98%, and maximum input power of 130W (12V voltage) (EPEVER, 2022a). The other controller is the tracer 1206AN model, with characteristics equal to the four characteristics cited of the TRIRON 1206N controller (MPPT algorithm, MPPT efficiency, maximum DC-DC conversion, and maximum input power) (EPEVER, 2022b). The differences between the two controllers are slight, being restricted to the existence of aUSB output with 5V voltage in the TRIRON 1206N model, which can charge electronic devices, and the location of the RS485 communication module, which is different on both controllers.

Fig. 5. Battery Heliar Freedom DF300

The fixed system used two LED lamps of the Brand Sorte Lux, with a voltage of 12V and power of 10.5W, with an estimated service life of 25,000 hours, making an installed power of 21W. The system with manual tracker used three lamps of the Brand G-Light, with a voltage of 12V and power of 8W, the service life of 25 thousand hours, and a total power load of 24W. In the final phase of the experiment, a 10.5W lamp of Sorte Lux (same model as the fixed system) was added to the system with the manual tracker to spend the additional energy generated by the 3-position system per day, preventing the battery from being charged and preventing the photovoltaic system from operating outside the MPPT point. The lamps used are shown in Figure 6.

Fig. 6. 10.5 W and 8 W power lamps used in the experiment

The fixed system and the solar tracking system used identical electrical protection equipment. The electrical protective boxes are located inside the masonry room and consist of a fuse, DC circuit breaker, and DC surge protection device (figure 7). In each system, a Unipolar 6A CC circuit breaker, of the Horel brand, in addition to a DPS CC of the Tomzn brand, with 1000 V of nominal voltage, 40 kA of maximum discharge current, and 20 kA of rated discharge current (MAGAZINE LUIZA, 2022) was used. The two DPS were interconnected in the same grounding rod, located outside the masonry room. Additional circuit breakers have been installed between the charge controllers and the batteries.

Fig. 7. Electrical protective box

Solar radiation measurement was performed through the pyranometer (figure 8) installed in funceme's PCD station, located in UECE, Kipp&Zonen brand, model CMP3. It is located 85 meters away from the two photovoltaic modules of the experiment. The CMP3 pyranometer (ISO 9060: 1990 Second Class) measures global shortwave solar radiation in the spectral range from 300 to 2800 nm (KIPP&ZONEN, 2022). The thermostat detector meters irradiance up to 2000 W/m² with a response time <18 seconds and typical sensitivity of 10 µV/W/m². The electrical energy generated by the two solar modules of the study was measured using the DC wattmeter model PZEM-031, brand OEM. Its operating range is between 6.5 V and 100 V voltage, 0 to 20 A current, and 0 to 9,999 Wh of power, with an accuracy of ± 1% (SOL E AR, 2022). It is located before the input of the chargecontroller.

Fig. 8. Kipp & Zonen CMP3 Piranometer

The DC wattmeter model PZEM-031 has LCD screen and accumulates measured electrical power data even when the screen is off and is not receiving electricity from the source. In addition to measuring the electricity generated, it reports power, voltage, and current data. Figure 9 has an illustration of the PZEM-031 wattmeter:

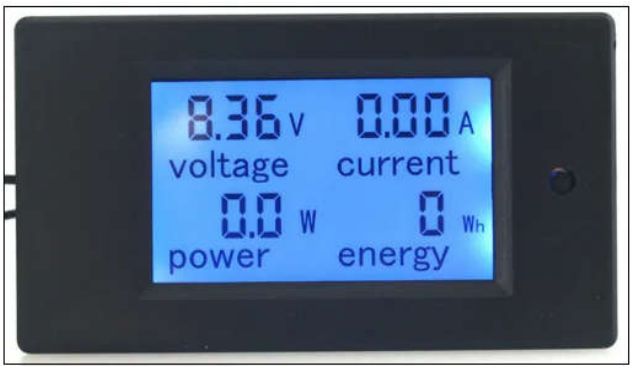

Fig. 9. Wattmeter PZEM-031

Datalogger eLOG01 (Figure 10) of the EPEVER brand is of the same mark as the two charge controllers of the design. Each Load Controller was connected to a datalloger eLOG01 via an RS485 cable for data transmission, so there were two datallogers used in the study. In addition, the power supply was also performed through the RS485 cable. The average energy consumption is in the order of 0.3Wh.

Fig. 10. Datalloger EPEVER eLOG01

The results stored on the datalloger eLOG01 are transmitted to a PC or Notebook via a USB communication cable model CC-USB-USB-150U. It accumulates data every 10 minutes on the electrical power generation of the photovoltaic module, on the battery, and the consuming charge of electricity (LED lamps). The storage capacity is 20,000 measurements (BIMBLE SOLAR, 2022). The PZEM-031 wattmeter was necessary, even with the datalloger eLOG01, due to the distinct precision of the two devices for measuring the electrical energy generated by the photovoltaic module. The eLog01 only measures 0.27 kWh, for example, the PZEM-031 wattmeter can measure 273 Wh, for example, which is equivalent to 0.273 kWh, so the wattmeter is more accurate. Next, in Figure 11, we have a panoramic view of the electrical structure mounted inside the masonry room:

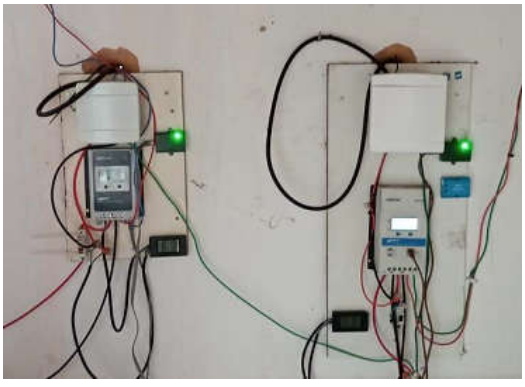

Fig. 11. Electrical structure built in the masonry room

The study compared the performance of two photovoltaic systems of the same installed power (50 W_p), one with a fixed angle of 0º in the horizontal plane and the other with various inclinations through a manual solar tracker, with the mechanical axis rotating between 45º East and 45º West, in the city of Fortaleza, located in the state of Ceará, Brazil. The system with a solar tracker has no south-north tilt. The fixed system is not self-cleaned by rain, so the two systems were cleaned daily for the comparison to be as accurate as possible. Electrical wires connected each photovoltaic module to a distinct DC wattmeter, where the energy generated was measured. Each DC wattmeter is then connected to a 10A charge controller. Then each charge controller was connected to a separate battery, a charge of LED bulbs, and a datalogger. The experiment was designed for the two systems to work at the maximum power point at 100% of the comparative time. For this to happen, the lamps were always on during the day, spending the energy generated from photovoltaic modules, only turning off at night, when the modules were not generating, and the battery voltage fell below the minimum voltage level programmed by the chargecontroller. When this minimum voltage level was reached, the controller automatically turned off the lamps.

The battery started the day discharged, and in the hours of greatest solar radiation it stored the energy generated by the modules, the value that exceeded the instantaneous consumption of the lamps. While the fixed system had an installed load of lamps with a power of around 21W, at times close to noon, on clear days, it was common for the fixed system power visualized on the wattmeter to reach 45W or more. Datalogger stored the data provided by the chargecontroller, at a frequency of 11 minutes, the periodicity that came factory scheduled in the datalloger. Data provided by datalloger were varied, such as voltage, current, and power of the electric charge, photovoltaic modules, and battery. They were seen in an Excel spreadsheet after connecting a USB cable to a Notebook. The primary function of each datalloger was to confirm that each photovoltaic module was running at 100% of the working time at the maximum power point, with the battery charge status column showing the information "raising charge". In preliminary tests, before the experiment, when the battery increased energy storage and the lamps were turned off manually, the battery charge status column showed other information such as "float charge," for example. The irradiation value in the horizontal plane, obtained by the PCD-FUNCEME station, were informed via e-mail through an Excel spreadsheet, with data periodicity of 60 minutes. Data collection from the datalloger was always performed twice, once at the beginning and once at the end of each stage of study collection. Data on the energy generation of the systems were obtained daily, after 5:30 pm, with the sky darkening, through a photo of each wattmeter, at the moment the value of the generated electric current reached zero in the device.

The work was carried out in three stages. The first stage compared the system with a fixed angle of 0º in the horizontal plane (azimuth 0°, tilt 0°) with the system with a manual solar tracker with the exact angle of the fixed system. This comparison evaluated possible generation differences caused by the extension of electrical cables, the different chargecontrollers, and photovoltaic modules since the manufacturers recognize in the technical specifications that the modules may have a real power slightly higher or slightly lower than the official rated power. Considering the difference in electrical generation pointed out in comparing the two systems with the same angle, the comparative values of the following two stages became more reliable. This comparison was made for six consecutive days, starting on 07/28/2021 and ending on 08/02/2021. The second stage occurred through a comparison between the system with an angle of 0º in the horizontal plane throughout the day, and the photovoltaic system with a manual tracker with two daily positions, positioned at the 45º East angle (azimuth 90°, tilt 45°), during the morning until noon. The reference used was the solar noon for the city of Fortaleza, the noon of the official time was not used. Exactly the minute the solar noon was reached, the photovoltaic module with a manual tracker was positioned at the 45º West angle (azimuth -90°, tilt 45°).

Around 6:00 p.m., the module was back in position 45° East, the same position of other day in the morning. A human operator made the tracker changes. The operator had no difficulty obtaining the two angles because the end of the course of the manual tracker axis was precisely at the 45º angle, both in the West and East direction. The choice of the 45º angle was because the city of Fortaleza is located very close to the Equator line. In the equinoxes, the position of 45º of the photovoltaic module achieves maximum direct radiation in the middle of the morning and the middle of the afternoon. Thus, the misalignment of the angle of incidence with the normal of the photovoltaic module plane does not exceed 45º on any day of the year concerning the angle of the solar height, avoiding drastic losses of incidence of solar radiation because of the misalignment of the module at the beginning of the day and in the solar noon. The comparison of the second stage was carried out for five days in a row, starting on 08/04/2021 and ending on 08/08/2021. The third stage was performed by comparing the system with an angle of 0º in the horizontal plane throughout the day and the photovoltaic system with a manual tracker with three daily positions. As the existing structure of the manual tracker with a final stroke with a 45º angle was used, it was not considered to use a more inclined angle. The tracker system always started the day at an angle of 45º East. Exactly 1h30min before noon solar, a human operator changed the angle to 0º in the horizontal plane. A piece of wood was placed on the shaft to stabilize the board at the angle, and then the angle was confirmed with a level gauge. Exactly 1h30min after solar noon, a human operator changed the angle of the manual tracker to 45º East. Around 6:00 p.m., the module was back in position 45° East, which would begin the other day in the morning. The comparison of the third stage was performed for five days in a row, starting on 08/11/2021 and ending on 08/15/2021. In the first and third stages, the two systems were compared in terms of the daily electric energy (E_{ed}) generated in Wh. It is achieved by integrating the instantaneous electrical power (Pot) in watts, over time (t) in seconds. The integration mentioned in equation 2 is performed by the PZEM-031 wattmeter. The resulting value in joules is then converted to Wh:

$$E_{ed} = \int_{day} Pot_e \, .dt \quad (2)$$

In the second stage, which contained the main objective of the experiment, the comparison between a fixed system and a system of two daily positions, in the city of Fortaleza, was compared the daily electric energy (E_{ed}) generated, and the capacity factor (CF) of the two systems. The value of the daily irradiation in the horizontal plane was obtained in the five days of the second stage, in kWh/m². In addition, another four indicators were obtained from the fixed system at 0º in the horizontal plane (reference productivity, PV arrangement productivity, PV arrangement efficiency and performance ratio). The following will be presented to the formulas of some indicators measured in the second stage. The yields of a photovoltaic arrangement show the actual operation of the photovoltaic arrangement compared to its nominal capacity. The reference productivity (Y_R) (equation 3) is the division of global horizontal irradiation (H_T) in the plane by reference irradiance (H_R). The value of H_R is 1 kW/m² (VIDAL; DE LIMA, 2020, p. 34198). Reference irradiance represents a measure of theoretical energy available in one place in a given period.

$$Y_R = \frac{H_T}{H_R}\left(\frac{kWh}{kW_P \, .day}\right) \quad (3)$$

The productivity of the photovoltaic arrangement (Y_{FV}) (equation 4) is the direct current energy output (E_{CC}) of the photovoltaic arrangement expressed in Wh over some time, divided by the nominal power of the photovoltaic modules (P_{FV}). It expresses the time that the photovoltaic matrix must operate with its rated power to generate the energy produced by the photovoltaic arrangement. The experiment's direct current energy output (E_{CC}) is the daily electrical energy (E_{ed}) generated in equation 2, measured by the PZEM-031 wattmeter.

$$Y_{FV} = \frac{E_{CC}}{P_{FV,nom}}\left(\frac{kWh}{kW_P \, .day}\right) \quad (4)$$

The performance ratio (PR) consists of the relationship between a photovoltaic system's actual and theoretical energy outputs. It shows the proportion of electrical energy available to the electricity grid after the operation losses, such as those caused by heating the modules, electrical cables and converting the energy of the inverter or charge controller. The performance ratio is calculated by equation 5 (DE LIMA *et al*., 2017, p. 81):

$$PR = \frac{Y_F}{Y_R} \; x\,100\% \quad (5)$$

In equation 5, the $Y_R$value represents the reference productivity mentioned in equation 3. The Y_F value is the final productivity (equation 6), defined as the total AC energy produced by the photovoltaic arrangement divided by the nominal power of the photovoltaic system. In the present study, it was impossible to calculate the final productivity's exact value because datalogger eLOG01 does not provide this information. The value of the performance ratio was simulated, using the values of the study of Morais (2017, p. 74) in August 2017, as a reference, the ratio between the productivity of the photovoltaic arrangement (Y_{FV}) of 5.17 kWh/kWp.day, and the final productivity (Y_F) of 4.99 kWh/kWp.day, in the month, mentioned. The choice of data for August was the same month where the collections of the present study occurred, with the distinction that they took place in different years (2017 and 2021). In the simulation, it was considered that the losses of the load controller EPEVER were the same as the inverter of the study of Morais (2017). Thus the final productivity value (Y_F) was obtained by multiplying the productivity value of the photovoltaic arrangement (Y_{FV}) by 0.965 (4.99/5.17).

$$Y_F = \frac{E_{CA}}{P_{FV,nom}}\left(\frac{kWh}{kW_P \, .day}\right) \quad (6)$$

The capacity factor (CF) means the ratio between the total AC power generation produced in a given period, which can be a day, month, or year, and the amount of energy that the photovoltaic arrangement would generate if it operated at a total rated power ($P_{FV,nom}$) during the total designated period. In equation 7, a period of 24 hours per day in a whole year (8,760 hours) is used as a reference. The capacity factor (CF) value was also simulated from the multiplication of the direct current energy output value (E_{CC}), measured by the PZEM-031 wattmeter by 0.965, considering the same losses of of the study of Morais (2017) mentioned in the previous paragraph. The capacity factor was simulated in the fixed system and the system of two daily positions with the manual photovoltaic tracker.

$$CF \; = \frac{E_{CA}}{P_{FV,nom} \, X \, 8{,}760} \quad (7)$$

The efficiency of the photovoltaic arrangement (η_{FV}) is given in percentage (equation 8). It means the average energy conversion efficiency of the photovoltaic arrangement, which is the ratio between the daily generation of DC energy and the product of total daily irradiation in the plane (H_T) in an area corresponding to the area of the photovoltaic arrangement (A_{FV}) in m² (DE LIMA *et al*., 2017).

$$\eta_{FV} = \frac{1\;00X\;E_{CC}}{H_T \, X \, \text{AFV}} \; (\%) \quad (8)$$

Finally, two simulations were performed in the Radiasol 2 software (APB INSTALAÇÕES ELÉTRICAS, 2022), developed by the Federal University of Rio Grande do Sul (UFRGS). This software uses an international solar radiation database to simulate the average monthly incident radiation in several Brazilian cities in a given plane, with the possibility of changing the tilt of the plane. The first simulation makes a comparison very similar to that of the experiment's main objective, the comparison between the one fixed system and a system of two daily positions, in the city of Fortaleza, as to the annual incident radiation. The only difference is that instead of using the solar half day to change the position of the module, it was

used the half day of the official time. The second simulation altered the slope in the south-north direction, making no changes in the east-west direction. In the second simulation, an inclination of 18º South was added during 6 months of the year, and 18º North during another 6 months, configuring two annual changes.

RESULTS AND DISCUSSION

Data collected from solar irradiation, electricity generation, charge statuts and battery status were discussed in three stages.

FIRST STAGE

The first stage began on 07/28/2021 and ended on 08/02/2021, six days. The two 50 W_p modules were positioned without inclination, with a fixed angle of 0º in the horizontal plane. They functioned as identical systems, same installed power (50 W_p) and same slope in practice. The generation difference between the two systems may have been caused by factors such as the extension of electrical cables, the different charge controllers, or the difference in the manufacturing quality of photovoltaic modules, even if they are modules of identical specification. Another possible cause of the difference in the electrical generation is the possibility of shading at the end of the day of the fixed system by large trees located 40 meters away from the experiment. In comparing six days, the fixed system generated 4.7% less electrical energy than the system with the manual solar tracker, generating a total of 1,403 Wh, against 1,472 Wh of the system with the tracker. This difference showed a great constancy over days; on 07/28/2021, on the first day, the fixed system generated 191 Wh against 200 Wh of the system with a manual tracker, 4.5% less. On 07/29/2021, on the second day, the fixed system generated 210 Wh versus 221 Wh of the system with the tracker, 4.98% less. Figure 12 shows the graph with the average daily electricity (E_{ed}) generated in each system during the period:

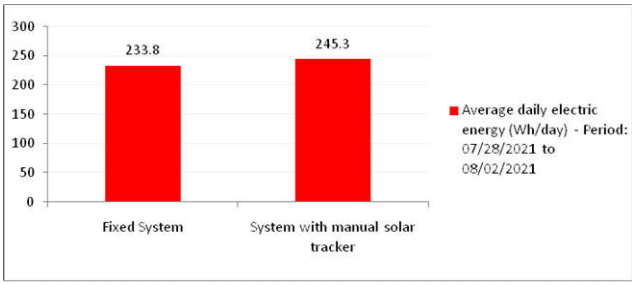

Fig. 12. Average daily electricity energy (Wh/day) in Stage 1, per system

SECOND STAGE

The second stage began on 08/04/2021 and ended on 08/08/2021, totaling five days. The second stage represented the most prominent object of study of the work, the comparison between the fixed system at 0º in the horizontal plane and a system of manual solar tracker of two daily positions in the city of Fortaleza, Ceará, positioned at the angle 45º East, from the beginning of the morning until the solar noon, and 45º West of the solar noon until the end of the day. In the 5-day comparison, the system with a manual solar tracker of two daily positions generated 29.97% more electricity than the fixed system, generating 1,652 Wh, against 1271 Wh of the fixed system. However, only 1,574.3 Wh of generation in the tracker system was considered because the value 1,652 Wh was multiplied by 0.953. This deduction was adopted because, in the first stage, the fixed system had a 4.7% lower generation under conditions similar to the system with the tracker. Then the system with a manual solar tracker of two daily positions generated 23.86% (1.299 x 0.953) more than the fixed system in 5 days. The data from the following comparisons already have the reduction of 4.7% adopted in the value of the electrical generation of the system with the solar tracker to avoid the need to repeat several times the value measured in the wattmeter and the value with the reduction of 4.7%. Figure 13 shows the graph with the average daily electricity (E_{ed}) generated in each system during the second stage:

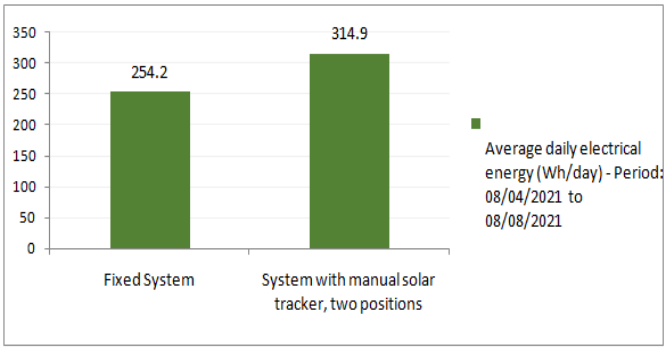

Fig. 13. Average daily electricity energy (Wh/day) in Stage 2, per system

The net gain of 23.86% increase in electricity generation, in the experiment carried out with the tracker of two daily positions compared to the fixed system in the city of Fortaleza, Ceará, was a gain very close to the gain achieved by the study by Huang and Sun (2007), which had an estimated generation increase of 24.5%, with a solar tracking system of 3 positions per day, of 1 axis, without concentration. This shows that a system with two daily positions can significantly increase electrical generation, with the cost benefit of requiring only two daily position changes. Table 1 shows the electricity generated in the fixed system and the system with manual tracking of two positions in each of the five days of the comparison of the second stage:

Table 1. Electricity generated (Wh) per day, in Stage 2

Day	1-Fixed system	2-tracker system	Increasein generation
1-08/04	257	325.9	26.8%
2-08/05	260	340.2	30.84%
3-08/06	243	275.4	13.33%
4-08/07	261	336.4	28.88%
5-08/08	250	296.3	18.52%

The increase in daily electricity generation caused by the tracker varied widely over five days, reaching a peak of 30.84% increase on 08/05/2021 and a floor of 13.33% on 08/06/2021. These variations can be justified by the proportion of direct irradiance in global irradiance on each day and in its distribution during the day. Days with clear skies during the hours near noon and cloudy skies at the beginning and end of the day favor the fixed system. Days with clear skies at the beginning and end of the day and cloudy skies in the hours near noon favor the system with the two-position daily solar tracker. This is because the angle of incidence of the sunbeam is less misaligned with the normal plane of the photovoltaic module of fixed system at noon. In contrast, the angle of incidence of the sunbeam is less misaligned with the normal of the photovoltaic module of the two-position tracker at 9 a.m. and 3 p.m. The daily irradiation incident in the horizontal plane on each of the five days of the second stage is available in Figure 14 from the data provided by FUNCEME. In the second stage, the daily average of solar irradiation was 6.31 kWh/m², with every day with solar irradiation above 6 kWh/m² (FUNCEME, 2022). On 08/05/2021, adding the incident radiation that occurred until 9 a.m. with the incident radiation from 3 p.m., the two values together represented 26.58% of the total irradiance of the day. In comparison, between 11 a.m. and 1 p.m., the incident radiation represented 25.92% of the total irradiance of the day. On 08/06/2021, this relationship was reversed, adding to the incident radiation that occurred until 9 a.m. with the incident radiation from 3 p.m., the two values together represented 23.69% of the total irradiance of the day. In comparison, between 11 a.m. and 1:00 p.m., the incident radiation represented 27.85% of the total irradiance of the day. This difference helped the tracker system to obtain the most

significant increase in power generation on 08/05 and the smallest increase on 08/06.

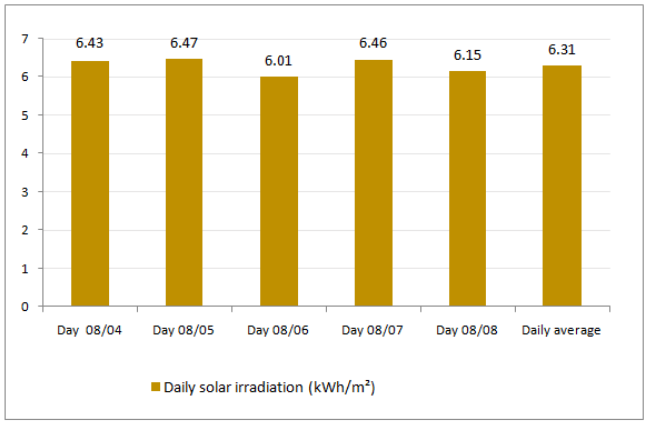

Fig. 14. Solar irradiation per day – Stage 2 (FUNCEME PCD station)

.

The following are four indicators obtained from the fixed system at 0º in the horizontal plane (reference productivity, productivity of the photovoltaic arrangement, efficiency of the photovoltaic arrangement and performance ratio), considered the reference system of the comparison, in each of the five days. The reference productivity (Y_R) and the productivity of the photovoltaic arrangement (Y_{FV}) did not have significant variations during the five days of the comparison. The mean reference productivity (Y_R) was 6.31 kWh/kW$_p$.day, while the average productivity of the photovoltaic arrangement (Y_{FV}) was 5.08 kWh/kW$_p$.day in the period. The complete data per day is shown in Figure 15:

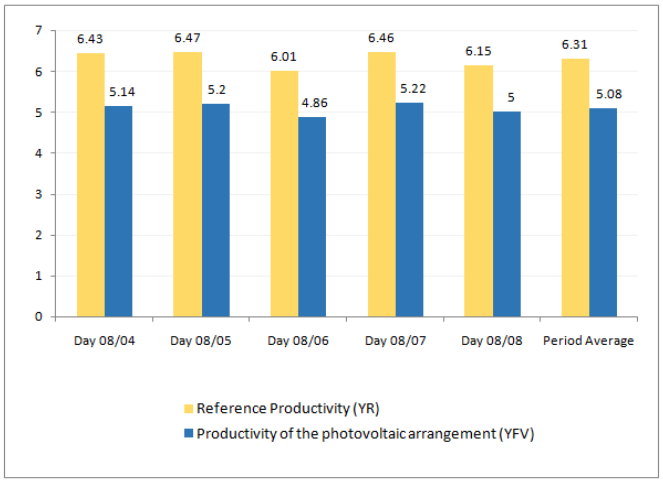

Fig. 15. Productivities values per day - Stage 2, fixed system of 50 W$_p$

For comparison, in the study of Morais (2017), the average reference productivity (Y_R) in August 2017 was 6.46 kWh/kWp.day, while the average productivity of the photovoltaic arrangement (Y_{FV}) in August 2017 was 5.17 kWh/kWp.day, a 2.3% higher value of Y_R, and a 1.7% higher value of Y_{FV} compared to the present experiment, also held in August, but four years later (year 2021), and in only five days. The differences were minimal between the two studies. The Morais system (2017) is located only 40 meters away from the experiment but has distinct angles, azimuth 25°, and tilt 8°; these differences may have impacted the results. The study by Morais (2017) evaluated a photovoltaic system of 5.2 kW$_p$ connected to the public electricity grid through an inverter with MPPT. The performance ratio (PR) had slight variations in the fixed reference system during the five days of the experiment. The value of the performance ratio was simulated, as mentioned in the Materials and Methods section, using the values of the work of Morais (2017, p. 74) in August 2017 as a reference. The relationship between the productivity of the photovoltaic arrangement (Y_{FV}) of 5.17 kWh/kWp.day and the final productivity (Y_F) of 4.99 kWh/kWp.day, in the month cited. The choice of data for the month of August was due to the fact that it is the same month as the present study, with the distinction that they took place in different years (2017 and 2021). In the simulation, it was considered that the final productivity value (Y_F) applied in the formula of equation 5 was obtained by multiplying the productivity value of the photovoltaic arrangement (Y_{FV}), contained in figure 15, by 0.965 (4.99/5.17). The mean value of the performance ratio (PR) was 77.7%. The daily data are in Figure 16:

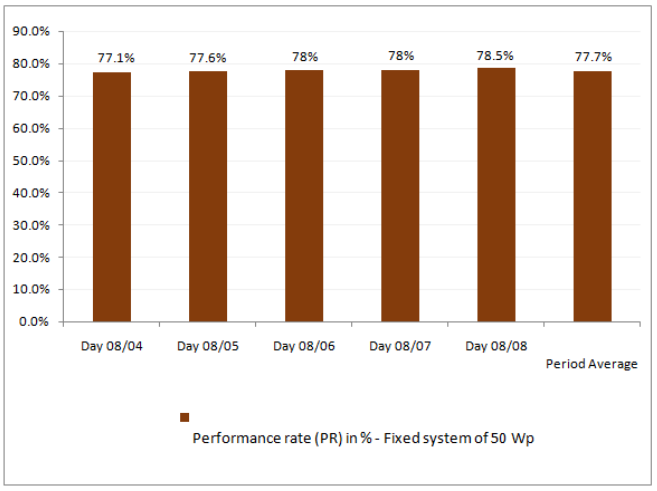

Fig. 16. Performance ratio (PR) per day - 2nd Stage, fixed system of 50 W$_p$

The efficiency of the photovoltaic arrangement (ηFV) is given in percentage, representing the average efficiency of energy conversion of the photovoltaic arrangement. The values also did not show significant variations in the fixed reference system during the five days of the 2nd Stage. The daily generation of DC energy values was extracted from Table 2. The total daily irradiation values in the plane were obtained from Figure 14. Furthermore, the photovoltaic arrangement area (A_{FV}) in m² of the Komaes KM50 photovoltaic module was 0.3825 m², calculated from the module dimensions. The mean efficiency of the photovoltaic arrangement (ηFV) was 10.5% in the period. The data per day is contained in Figure 17:

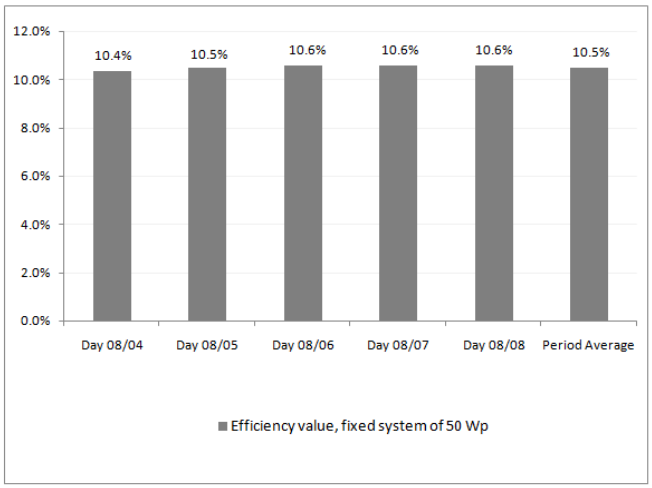

Fig. 17. Efficiency value (ηFV) per day - 2nd Stage, fixed system of 50 W$_p$

The capacity factor (CF) is the relationship between the total AC power generation produced in a given period and the amount of energy that the photovoltaic arrangement would generate if it operated at a total rated power ($P_{FV,\ nom}$) during the total period

designated, in this case, the 24 hours was used. The capacity factor (CF) value was also simulated from the multiplication of the direct current energy output value (E_{CC}), measured by the PZEM-031 wattmeter by 0.965, considering the same work losses of Morais (2017), used in the calculation of the performance ratio (PR). The capacity factor was simulated in the fixed system and the system of two daily positions with the manual solar tracker. The mean capacity factor (CF) value of the system with the manual solar tracker in 5 days was 26.2%, a significantly higher value than that of the fixed system, which was 21.2%. The daily results are shown in Figure 18:

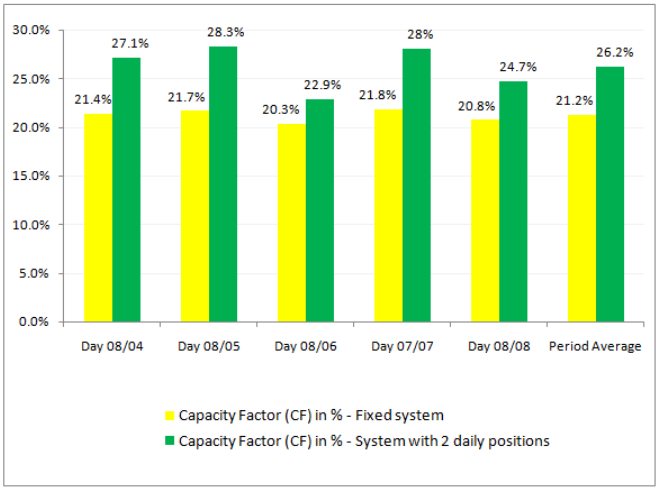

Fig. 18. Capacity factor (CF) per day - 2nd Stage, in the 2 systems

THIRD STAGE

The third Stage began on 08/11/2021 and ended on 08/15/2021, totaling five days. The two systems had the same power (50 W_p), but one had an angle of 0º in the horizontal plane throughout the day. At the same time, another consisted of a photovoltaic system with a manual tracker with three daily positions. The tracker system always starts the day at an angle of 45º East, and 1h30min before noon solar, a human operator changes the angle to 0º in the horizontal plane. Then, 1h30min after noon solar, a human operator changed the angle of the manual tracker to 45º East. In the 5-day comparison, the system with a manual solar tracker of three daily positions generated 36.3% more electricity than the fixed system, generating 1,690 Wh, against 1,240 Wh of the fixed system. However, only 1,610.6 Wh of generation in the tracker system was considered because the value 1,690 Wh was multiplied by 0.953. This deduction was adopted because, in the first stage, the fixed system had a 4.7% lower generation under conditions similar to the system with the tracker. Then the system with a three-position daily tracker generated 29.89% (1.363% x 0.953) more than the fixed system in the five days. Figure 19 shows the graph with the average daily electricity (Eed) generated in each system during the 3rd Stage:

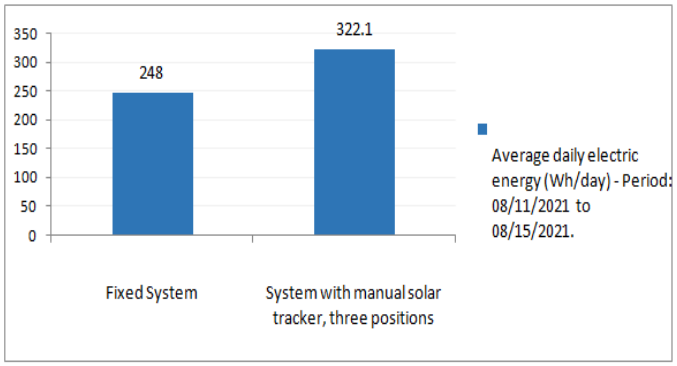

Fig. 19. Average daily electricity energy (Wh/day) in Stage 3, per system

SIMULATIONS WITH RADIASOL 2 SOFTWARE

The Radiasol 2 Software (APB INSTALAÇÕES ELÉTRICAS, 2022) was developed by the Federal University of Rio Grande do Sul (UFRGS). It calculates solar radiation on sloping surfaces through operations involving trigonometric calculations and models of historical solar radiation data's temporal and spatial distribution. Location data, location albedo, azimuthal deviation, and module slope are entered. All simulations considered the location of the city of Fortaleza and local albedo of 0.2. The first simulation made a comparison between a fixed system with azimuth 0° and tilt 0° (equal to the fixed system of the practical experiment) and a system with two daily positions, with azimuth 90° and tilt 45°, during the morning until noon, and azimuth -90° and tilt 45°, from noon to late afternoon. The two-position daily system simulated in Radiasol 2 was very similar to the manual solar tracker system of the practical experiment of two daily positions. The only difference was the use of official time, solar time was not used, which generated a small difference of approximately 10 minutes from the moment of change of inclination. The Radiasol 2 software has a database provided from the official time, so this was the only option to use. The program interface is shown in figure 20, with the data entered in the simulation of the fixed system.

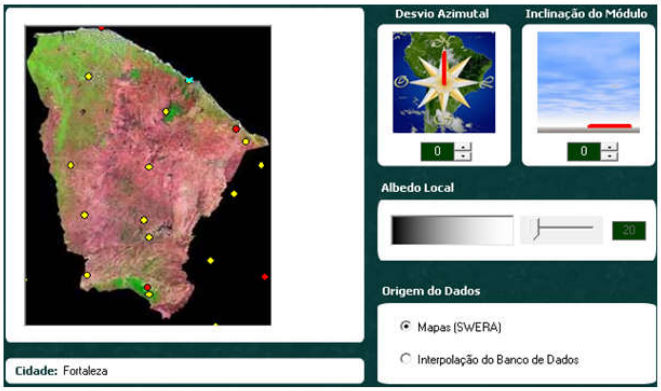

Fig. 20. Radiasol 2 Program, with the data entered from the fixed system

The average annual irradiation in Fortaleza was 5.51 kWh/m²/day in the fixed system. In the system of two daily positions, two data inserts were performed. The first with azimuth 90° and tilt 45°, accounting for incident irradiation until noon, considering the average hourly radiation each month. In the second insertion, the azimuth -90° and tilt 45° were used, accounting for the incident irradiation from noon to the end of the day, considering the average hourly radiation each month. Figure 21 shows the simulation data with azimuth 90° and tilt 45°, provided per month and per hour by the Radiasol 2 program.

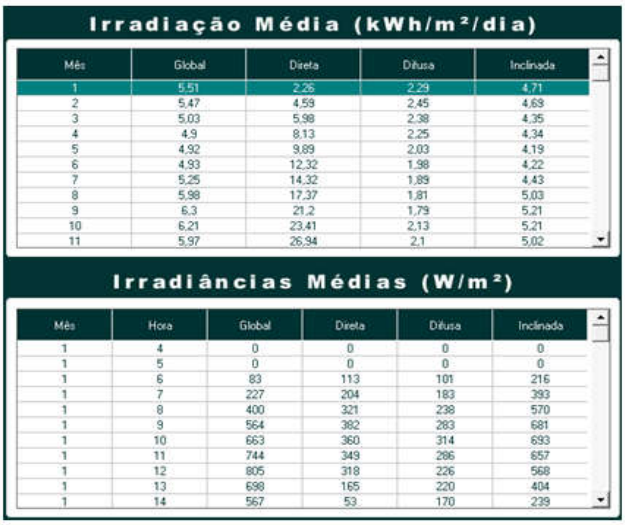

Irradiação Média (kWh/m²/dia)

Mês	Global	Direta	Difusa	Inclinada
1	5,51	2,26	2,29	4,71
2	5,47	4,59	2,45	4,69
3	5,03	5,98	2,38	4,35
4	4,9	8,13	2,25	4,34
5	4,92	9,89	2,03	4,19
6	4,93	12,32	1,98	4,22
7	5,25	14,32	1,89	4,43
8	5,98	17,37	1,81	5,03
9	6,3	21,2	1,79	5,21
10	6,21	23,41	2,13	5,21
11	5,97	26,94	2,1	5,02

Irradiâncias Médias (W/m²)

Mês	Hora	Global	Direta	Difusa	Inclinada
1	4	0	0	0	0
1	5	0	0	0	0
1	6	83	113	101	216
1	7	227	204	183	393
1	8	400	321	238	570
1	9	564	382	283	681
1	10	663	360	314	693
1	11	744	349	286	657
1	12	805	318	226	568
1	13	698	165	220	404
1	14	567	53	170	239

Fig. 21. Radiasol 2 Program, given with azimuth 90° and tilt 45°

The average annual irradiation in Fortaleza was 6.6 kWh/m²/day in the system of two daily positions, a value 19.78% higher than the fixed system. When correlating this simulated value with the gain of 23.86% of the experiment performed (second stage), some questions need to be relativized. The first point is that the practical experiment was carried out for only five days (08/04/2021 until 08/08/2021), a short period, so it may have been greatly influenced by daily radiation dynamics different from those that happen on most days of the year, less cloudy mornings than the vast majority of days of the year, for example, while the simulation covered the whole year. Another point is that the daily average of irradiation in the five days was higher than the annual daily average indicated in Radiasol 2 for Fortaleza, a value of 6.31 kWh/m²/day against a value of 5.51 kWh/m²/day, which favored the system of the practical experiment. Suppose the 19.78% average daily irradiation gain indicated by the Simulation of the Radiasol 2 program is confirmed in the real world. In that case, this does not mean an equal increase in photovoltaic energy generation. More daily irradiation means a higher temperature of the modules during the day and more significant voltage drops by this factor.

However, even if the photovoltaic system generates 17% or 18% more in the real world than the fixed system, already discounting temperature losses, it will still be a relevant gain considering that only two daily position changes will be required. For comparison, the study of Gutierrez *et al*. (2020), held in Aguascalientes, Central Mexico, achieved a gain of 29.9% with a one-axis system compared to a fixed system during nine days of May 2020, using a complex internet of things technology to position the module. The second simulation in Radiasol 2 altered the tilt in the south-north direction, making no changes in the east-west direction. An 18º North tilt was inserted in the program(azimuth 0º, tilt 18º) was inserted during six months of the year (April, May, June, July, August, and September), and 18º South tilt (azimuth 180º, tilt 18º), during another six months (October, November, December, January, February, and March), configuring two annual changes. The tilt of 18º was chosen manually in the program, through many attempts, with the city of Fortaleza as a place, seeking the highest possible average radiation with two distinct annual positions, with entirely different azimuth and the same inclination. This simulation with two annual positions generated an annual average of 5.83 kWh/m²/day in the city of Fortaleza, a value 5.81% higher than the fixed system generated in the first simulation, 5.51 kWh/m²/day. As mentioned in the first simulation, this does not mean a 5.81% gain in photovoltaic generation in practice due to the loss by increasing the temperature of the modules due to higher incident radiation.

CONCLUSION

The comparison between the fixed system at 0º horizontally and the system of two daily positions with a 45º tilt on the east-west axis showed an excellent gain of 23.86% in electricity generation in the 5-day experiment in August 2021. This result, together with the annual gain of 19.78% of irradiation presented by the simulated system in the Radiasol 2 program, demonstrates that a two-position manual tracking system daily can be an excellent option for small and medium-sized microgeneration systems in distributed generation systems, where current tracking systems may not compensate, since in large systems a single engine moves an extensive shaft with dozens of photovoltaic modules at the same time, they are systems that need scale to be economically viable. The data evaluated exclusively in the fixed system, such as reference productivity, the productivity of the photovoltaic arrangement, the efficiency of the photovoltaic arrangement, and performance rate, served to verify whether the fixed system could be a good reference for the comparison with the system of two daily positions. The data collected proved that the fixed system has an excellent technical operating standard, with results compatible with those found in the literature. The system of 3 daily positions, with an electrical generation gain of 29.89% compared to the fixed system, presented a small additional gain compared to the system of two daily positions, not showing the same cost benefit.

In future works, one can build a prototype, with the two daily changes happening automatically, without human assistance. One can also evaluate a practical system with two daily positions, with azimuth of 45º and tilt of 18º in the morning and -azimuth of 45º and tilt of 18º in the afternoon, in the months close to June, to try to sum up the gains of the first Radiasol simulation with the gains of the second simulation. And so build a system with two daily positions following the Sun during the day, and having at the same time two annual positions in the south-north direction, to follow the orientation of the Sun in the seasons. As for the prototype, one possibility is to use a water system, where a water timer automatically fills a small reservoir to move the module to the East, and fills another small reservoir to move it to the West. And that this water can be reused, with the reservoir getting dry a few minutes after filling, which causes the module to rotate, while the system remains in position for several hours, through the aid of a magnet fastener. In the end, it can be considered that the results of the present study can be used in future experiments with a solar tracking system in the state of Ceará, Brazil.

Acknowledgments: Authors indebted to FUNCEME – Ceará State Foundation for Meteorology and Water Resources, for providing meteorological data.

REFERENCES

APB INSTALAÇÕES ELÉTRICAS. Programa Radiasol_2.0.rar. 2022. Available in: <https://drive.google.com/drive/folders/1hYpK4VlBt78-YTuEqJdoGwM9PFwpYB4z>.

AWASTHI, Anshul *et al*.Review on sun tracking technology in solar PV system. Energy Reports, [s.l.], v. 6, p.392-405, nov. 2020. Elsevier BV. https://doi.org/10.1016/j.egyr.2020.02.004.

BIMBLE SOLAR. Tracer Epever ELOG01 Data Logger. 2022. Available in: <https://bimblesolar.com/epever-elog1>.

CASTANEDA, César Eduardo Figueroa. Desenvolvimento de um rastreador solar passivo por transferência de massa. 2011. 94 f. Dissertação (Mestrado) -

Programa de Pós-Graduação em Desenvolvimento de Tecnologia, Instituto de Tecnologia para o Desenvolvimento (LACTEC), Curitiba, 2011. Available in: <https://lactec.org.br/wp-content/uploads/2021/03/PRODETEC-SERGIO-2013-07-15.pdf>.

DA SILVA, Tiago Venturini. Análise de eficiência de um seguidor solar em sistema conectado à rede: viabilidade econômica. Dissertação (Mestrado) -

Programa de Pós-Graduação em Energia, Universidade Federal do Espírito Santo, São Mateus, 2017. Available in: <https://repositorio.ufes.br/bitstream/10/8444/1/tese_11248_58-Tiago%20Venturini%20da%20Silva.pdf>.

DE LIMA, L. C. *et al*. Performance analysis of a grid connected photovoltaic system in northeastern Brazil. Energy for Sustainable Development,[s.l.], v. 37, p.79-85, 2017.Elsevier BV. https://doi.org/10.1016/j.esd.2017.01.004.

DE SÁ CAMPOS, Manoel Henrique; TIBA; Chigueru. NpTrack: A n-Position Single Axis Solar Tracker Model for Optimized Energy Collection.Energies, v. 14, p.1-13, 2021. https://doi.org/10.3390/en14040925.

EPE (EMPRESA DE PESQUISA ENERGÉTICA). Anuário Estatístico de Energia Elétrica 2011.2011. Available in: <https://www.epe.gov.br/sites-pt/publicacoes-dados-abertos/publicacoes/PublicacoesArquivos/publicacao-160/topico-168/Anu%C3%A1rio%20Estat%C3%ADstico%20de%20Energia%20El%C3%A9trica%202011.pdf>.

EPE (EMPRESA DE PESQUISA ENERGÉTICA). Balanço Energético Nacional 2017: Relatório Síntese.2017. Available in: <https://www.epe.gov.br/sites-pt/publicacoes-dados-abertos/publicacoes/PublicacoesArquivos/publicacao-46/topico-81/S%C3%ADntese%20do%20Relat%C3%B3rio%20Final_2017_Web.pdf >.

EPE (EMPRESA DE PESQUISA ENERGÉTICA). Projetos fotovoltaicos nos leilões de energia: Características dos empreendimentos participantes nos leilões de 2013 a 2018.2018. Available in: <https://www.epe.gov.br/sites-pt/publicacoes-

dados-abertos/publicacoes/PublicacoesArquivos/publicacao-265/topico-417/EPE-DEE-NT-091_2018-r0.pdf >.

EPE (EMPRESA DE PESQUISA ENERGÉTICA). Anuário Estatístico de Energia Elétrica 2021.2021. Available in: <https://www.epe.gov.br/sites-pt/publicacoes-dados-abertos/publicacoes/PublicacoesArquivos/publicacao-160/topico-168/Anu%C3%A1rio_2021.pdf>.

EPEVER. TRIRON Series Modular MPPT Solar Charge Controller. 2022a. Available in: <https://epsolarpv.de/wp-content/uploads/2021/01/Datenblatt-Triron-Englisch.pdf>.

EPEVER. Tracer-AN series MPPT solar charge controller. 2022b. Available in: <https://epsolarpv.de/wp-content/uploads/ 2021/01/ Datenblatt-TracerAN-10-40A-Englisch.pdf>.

FUNCEME. Dados Meteorológicos da PCD FUNCEME/UECE durante o ano de 2021. [mensagem pessoal]. 2022. Mensagem recebida por <carire48@yahoo.com.br>.

GREENVOLT. O que sua construção precisa para receber o solar fotovoltaico. 2022. Available in: <https://greenvolt.com.br/o-que-sua-construcao-precisa-para-receber-o-solar-fotovoltaico/>.

GUTIERREZ, Sebastian*et al*. Development and testing of a single-axis photovoltaic sun tracker through the internet of things.Energies, v. 13, p.1-19, 2020. https://doi.org/10.3390/en13102547.

HAFEZ, A. Z.; YOUSEF, A. M.; HARAG, N. M.Solar tracking systems: Technologies and trackers drive types – A review. Renewable and Sustainable Energy Reviews, [s.l.], v. 91, p.754-782, ago. 2018. Elsevier BV. https://doi.org/10.1016/j.rser.2018.03.094.

HUANG, B. J.; SUN, F. S. Feasibility study of one axis three positions tracking solar PV with low concentration ratio reflector. Energy Conversion and Management, [s.l.], v. 48, p.1273-1280, abr. 2007. Elsevier BV. https://doi:10.1016/j.enconman.2006.09.020.

IPCC. Sixth Assessment Report: Chapter 6. 2022. Available in: <https://report.ipcc.ch/ar6wg3/pdf/IPCC_AR6_WGIII_FinalDraft_Chapter06.pdf>.

IRENA. Electricity storage and renewables: Costs and markets to 2030. 2017. Available in: <https://www.irena.org/-/media/Files/IRENA/Agency/Publication/2017/Oct/IRENA_Electricity_Storage_Costs_2017.pdf >.

KIPP&ZONEN. CMP3 Pyranometer. 2022. Available in: <http://www.kippzonen.com/Product/11/CMP3-Pyranometer#.WQjrGtrytPY>.

LIRA, José Rômulo Vieira. Desenvolvimento de um rastreador solar do tipo polar com ajuste de ângulo de inclinação. 2014. 65 f. Dissertação (Mestrado) -

Programa de Pós-Graduação em Engenharia Elétrica e de Computação, Universidade Federal do Rio Grande do Norte, Natal, 2014. Available in: <https://repositorio.ufrn.br/jspui/bitstream/123456789/15490/1/JoseRVL_DISSERT.pdf>.

MAGAZINE LUIZA. DPS - Dispositivo Proteção Surtos DC/CC 1000V/20KA / 40KA - TOMZN. 2022. Available in: <https://www.magazineluiza.com.br/dps-dispositivo-protecao-surtos-dc-cc-1000v-20ka-40ka-tomzn/p/ccjhff7h12/cj/dpdp/>.

MORAIS, Francisco Hedler Barreto de Lima. Análise de desempenho de um sistema fotovoltaico de 5,2 kW_pconectado à rede instalado na UECE. 2017. 95 f. Dissertação (Mestrado) - Curso de Mestrado Acadêmico em Ciências Físicas Aplicadas, Centro de Ciência e Tecnologia, Universidade Estadual do Ceará, Fortaleza, 2017. Available in: <https://www.researchgate.net /profile/Francisco_Hedler_Morais/publication/321862717_ANALISE_DE_DESEMP ENHO_DE_UM _SISTEMA_ FOTOVOLTAICO_DE_52_kWp_CONECTADO_ A_REDE_ INSTALADO_NA_UECE/links/5a35c995aca27247edde9cf3/ANALISE-DE-DESEMPENHO-DE-UM-SISTEMA-FOTOVOLTAICO-DE-5-2-kWp-CONECTADO-A-REDE-INSTALADO-NA-UECE.pdf?origin=publication_detail>.

NEOSOLAR. Bateria EstacionáriaHeliar Freedom. 2022. Available in: < https://www.loja.solarbrasil.com.br/MLB-1504877560-painel-placa-solar-fotovoltaica-50w-watts-padro-12v-komaes-_JM>.

OLIVEIRA, Maurício Madeira. Análise do desempenho de um gerador fotovoltaico com seguidor solar azimutal. 2008. 121 f. Dissertação (Mestrado) -

Programa de Pós-Graduação em Engenharia Mecânica, Universidade Federal do Rio Grande do Sul, Porto Alegre, 2008. Available in: <https://www.lume.ufrgs.br/handle/10183/14737>.

PEREIRA, Enio Bueno *et al*. Atlas Brasileiro de Energia Solar. 2017. Available in: <http://ftp.cptec.inpe.br/labren/publ/livros/Atlas_Brasileiro_Energia_Solar_2a_Edicao.pdf>.

PINHO, João Tavares; GALDINO, Marco Antonio (Org.). Manual de Engenharia para Sistemas Fotovoltaicos. 2014. Available in: <http://www.cresesb.cepel.br/publicacoes/download/Manual_de_Engenharia_FV_2014.pdf>.

QUASCHNING, Volker. Understanding Renewable Energy Systems. Londres: Earthscan, 2005. Available in: <http://www.beluco.net/references/quaschning-understanding.pdf>.

SOLAR BRASIL. Módulo Solar Fotovoltaico Komaes KM 50W. 2022. Available in: < https://www.loja.solarbrasil.com.br/MLB-1504877560-painel-placa-solar-fotovoltaica-50w-watts-padro-12v-komaes-_JM>.

SOL E AR. Wattimetro Voltimetro Amperimetro DC 100V 20A PZEM-031. 2022. Available in: <http://loja.solear.net.br/eletronicos/medidores/wattimetros/wattimetro-voltimetro-amperimetro-dc-100v-20a-pzem-031>.

SUMATHI, Vijayan *et al.*Solar tracking methods to maximize PV system output – A review of themethods adopted in recent decade. Renewable and Sustainable Energy Reviews, [s.l.], v. 74, p.130-138, jul. 2017. Elsevier BV. http://dx.doi.org/10.1016/j.rser.2017.02.013.

UFRGS. Tabela Trigonométrica. 2022. Available in: <http://www.ufrgs.br/biomec/materiais/Tabela%20Trigonometrica.pdf>.

VIDAL, Francisco Samuel Portela. Avaliação de desempenho de dois sistemas fotovoltaicos de bombeamento de água localizados na UECE. 2019. 95 f. Dissertação (Mestrado Acadêmico ou Profissional em 2019) - Universidade Estadual do Ceará, Fortaleza, 2019. Available in: <http://siduece.uece.br/siduece/trabalhoAcademicoPublico.jsf?id=83478>.

VIDAL, Francisco Samuel Portela; DE LIMA, Lutero Carmo. Performance evaluation of two pv water pumping systems in the state of Ceará, Brazil.International Journal of Development Research, v. 10, p.4195-34203, mar. 2020.

ZILLES, Roberto et al. Sistemas Fotovoltaicos Conectados à Rede Elétrica. São Paulo: Oficina de Textos, 2012. 208 p.

ZHONG, Hao*et al.*Optical performance of inclined southenorth axis three-positions trackedsolar panels. Energy, [s.l.], v. 36, p.1171-1179, feb. 2011. Elsevier BV. https://doi.org/10.1016/j.energy.2010.11.031.

****